Transactions, **SMiRT-25**
Charlotte, NC, USA, August 4-9, 2019
Division XI

LEAK TEST ON POLYUREA LINING POOL WALL AGAINST SEISMIC AND ACCIDENTAL LOAD

Yoshiro Manabe[1], Yoshihisa Ninomiya[1], Yusuke Kajiwara[1], Teruhito Urabayashi[2], Ryosuke Okunaka[2], Mitsuhiro Iwasaki[2], Minoru Yoshimoto[3], Tetsuya Asano[3], Hideyoshi Watanabe[4], Shin-ichi Takezaki [4], Hideo Ono[5], Masako Hiramatsu[5]

[1] Plant & Maintenance Engineering Group Nuclear Power Division, The Kansai Electric Power Co., Inc., Japan
[2] Civil Engineering and Architecture Engineering Group Nuclear Power Division, The Kansai Electric Power Co., Inc., Japan
[3] Construction Planning Group Nuclear Power Division, The Kanden Plant Corporation, Japan
[4] Technology Center, TAISEI Corporation, Japan
[5] Nuclear Facilities Division, TAISEI Corporation, Japan

ABSTRACT

Facilities corresponding to severe accidents at nuclear power plants require water source facilities for cooling. Even in the case where this water source facility is provided outside the radiation control area, it is necessary to confirm its water tightness and earthquake resistance, and it is advantageous to use high-performance aromatic resin coating having strength and flexibility as measures against water leakage.

To verify the soundness of the pool walls waterproofed by this method at the earthquake or severe accident load, we made a test specimen of the pool wall and after the above painting was applied to the inside of the wall, the reversed cyclic loading test was carried out in the water filled condition. As a result, it was confirmed that water leakage did not occur even if the pit was subjected to a deformation larger than expected at that of the earthquake, and it was possible to secure the water tightness

INTRODUCTION

There are pits and tanks as an option to provide a water source inside the building, but pits are more advantageous in terms of space occupied by buildings. When the water source pit is made of reinforced concrete, in order to prevent water leakage from cracks, a lining made of stainless steel has conventionally been applied. However, in recently, high-performance aromatic resin coatings with strength and flexibility have been developed and are beginning to be used in equipment that needs to ensure water tightness.

Therefore, in our research, we make a test specimen of a water source pit composed of reinforced concrete walls, apply high-performance aromatic resin coating inside, put water inside, and horizontal deformation beyond the design phase was applied, and it was confirmed that water leakage did not occur even in ultimate state. In addition, the outer surface of the wall was photographed with a digital camera, the image was digitally processed to obtain data on the width and spacing of the crack, and the relationship between the horizontal deformation and the width of the crack was evaluated. Furthermore, simulation analysis of the loading test was conducted by nonlinear FEM analysis, and the effectiveness of the analysis method in evaluating elasto-plastic behavior was evaluated.

TEST PLAN

Specimen

Fig. 1 shows the shape and dimensions of the test specimen, and Fig. 2 shows the arrangement of the test section (plan view). The test specimen is a 1/5 scale box type wall of actual water storage pit with stiff top and base slab, and its shape and dimensions are a wall core length of 1700 mm × 2200 mm and an internal height of 1600 mm. The wall thickness (t) was set so that the maximum value of fiber stress due to the out-of-plane bending moment by water pressure was equivalent to that of the actual pit, the axial force of the wall was set to zero so that the crack width was larger than the actual structure.
Its rebar ratio was Ps = 0.64%. This value is slightly less than the actual structure. The inner surface of the wall and the upper surface of the base stub are applied with high-performance aromatic resin of 3.0mm thickness for the purpose of preventing water leakage from cracks.

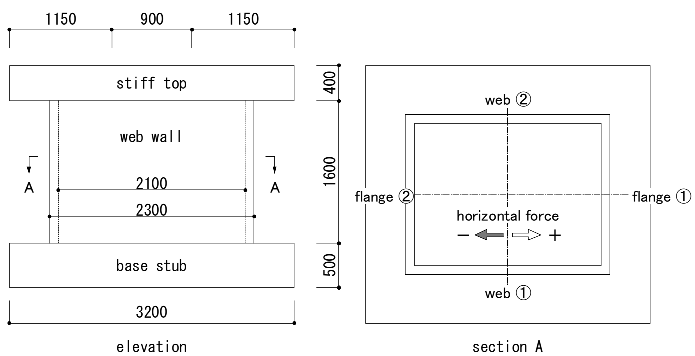

Fig.1 Shape and dimensions of the test specimen

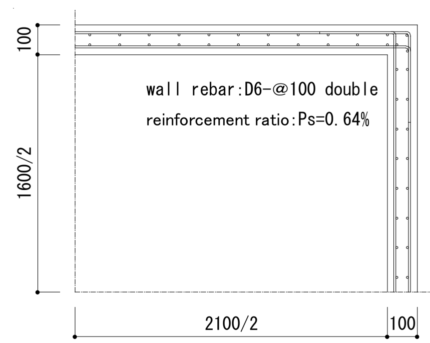

Fig.2 Rebar arrangement of wall

Material

Table 1 shows the material test results of concrete. The concrete used is plain concrete with a target compressive strength of 30 N / mm^2. The placing of concrete was done in three steps: base stub, test section and stiff top. Table 1 shows the average value of the concrete strength by 3 test pieces. Table 2 shows the result of material test of rebar. D6 (SD 345) was used for the wall rebar, main rebar D22 (SD 345) of the base stub and the stiff top and force distributing bar was D16 (SD 345), and D13 (SD 295 A) for the width fixing bar.

Table 1: Material properties of concrete

concrete	compressive strength (N/mm^2)	young's modulus ($\times 10^4$ N/mm^2)	poisson's ratio	split tensile strength (N/mm^2)
wall	33.0	2.95	0.21	2.87
base stub	36.7	3.01	0.20	3.34
stiff top	33.4	2.94	0.21	2.58

Table 2: Material properties of rebar

rebar		yield strength (N/mm^2)	young's modulus ($\times 10^5$ N/mm^2)	tensile strength (N/mm^2)	elongation (%)
wall	D6	388	1.83	599	23.0
basa stub stiff top	D22	374	―――	574	25.0
	D16	376	―――	572	25.2
	D13	358	―――	496	26.5

Measurement

The loading system is shown in Fig.3. Loading of horizontal force was performed by pushing and pulling four 2000 kN actuators attached to the top stiff stub with displacement control. The loading history is the same as in the previous test 1), and the total deformation angle R = ± 0.5 / 1000, ± 1/1000, ± 2/1000, ±

4/1000, ± 6/1000, ± 8/1000 twice each After a total of 12 cycles of reversed cyclic loading, the deformation angle was increased to R = 12/1000 to check the final condition. The measurements were carried out on shear force, total deformation, vertical section displacement in the test section to separate deformation components, rebar strain of wall. The loading set up is shown in Fig.4.

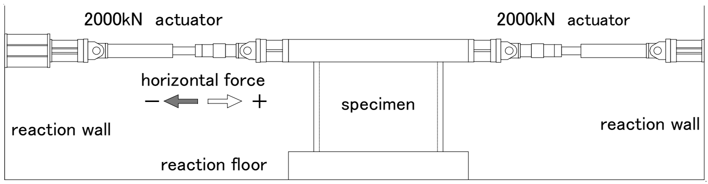

Fig.3 Loading system

Fig.4 Loading set up

TEST RESULTS

Crack Pattern

The crack pattern and the crack length-crack width relationship are shown in Fig.5 and Fig.6. The final crack patterns are shown in Fig.7. In this figure, the image taken with a high-precision digital camera is used as the input image, and the crack width is color-coded at a pitch of 0.2 mm for all the cracks that occurred.

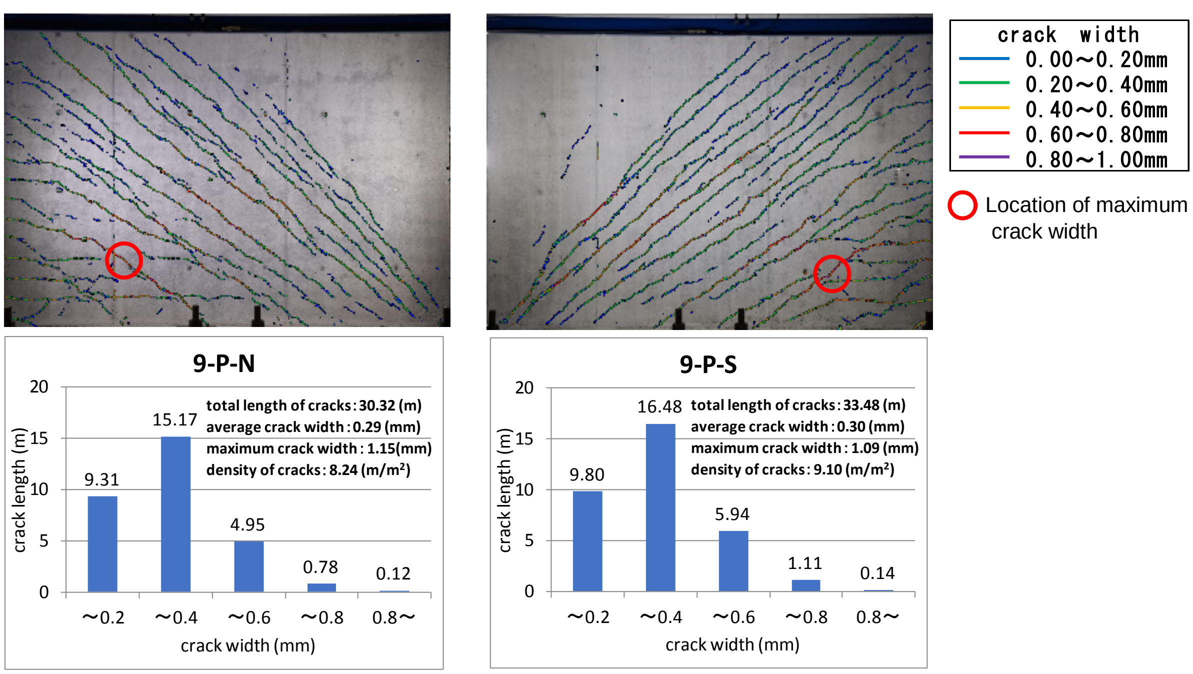

Fig.5 Crack pattern and crack length-crack width relationship (R=6/1000)

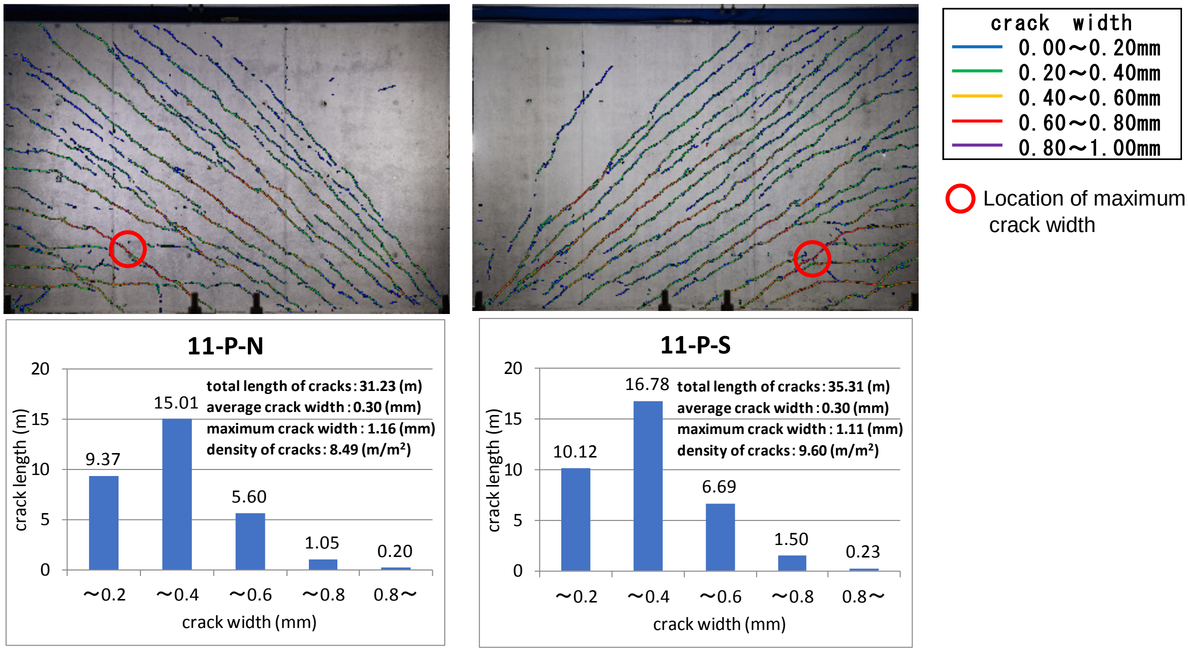

Fig.6 Crack pattern and crack length-crack width relationship (R=8/1000)

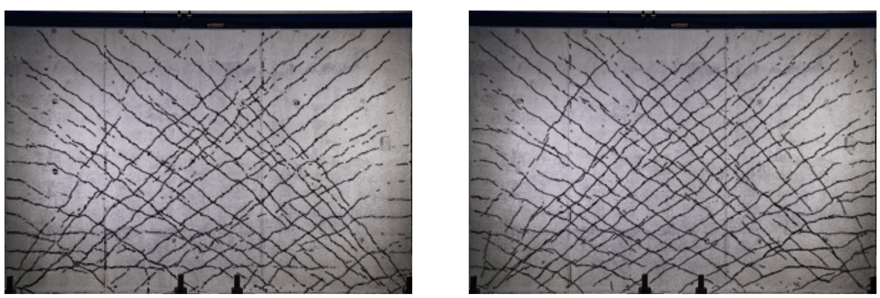

web①　　　　web②

Fig.7 Final crack pattern of web wall

The crack image analysis system of reference [1] was used. Fig.5 and Fig.6 show the cracks of the web walls at R = + 6/1000 and R = + 8/1000. In addition, the location of the maximum crack width is indicated by a red circle.

Bending cracks in the legs of the flange walls, with R = ± 0.5 / 1000, and in the center of the web walls with R = 1/1000 to 2/1000, large shear crack occurred. A long shear crack occurred at the center of the web walls. At deformation angles larger than this, many cracks occurred on the entire wall surface. The final crack spacing is about 100 mm, which is almost the same as the wall reinforcement spacing, which is the same result as previous researches [3] which examined the shear crack behavior of the shear wall.

As a result of dividing the total deformation angle R described later into a shear deformation (γ) and a bending deformation, the component of γ at R = ± 8/1000 is about γ = 5.5 to 6/1000. On the other hand, since the spacing of rebar in the specimen is 100 mm and is 1/2 of 200 mm of the actual wall, and from the previous research results [3], the final crack interval is equal to the rebar interval, the crack width of the test will be about half of the actual wall.

In addition, the allowable value of shear deformation angle (γ) in seismic design of nuclear facilities in Japan is 2/1000. The crack width of the wall of the actual wall which reached this γ is almost equal to the crack width of the test at the shear deformation angle of 4/1000. In this test, when the deformation angle

R reached 8/1000, the shear deformation angle γ exceeded 4/1000, but no water leakage from the crack was found for this deformation angle. In addition, when the deformation angle to be the final loading step is 12/1000, a vertical crack indicating crush of concrete occurs in the legs of surface of the compression side flange wall. Then, some peeling of concrete is occurred, but water leaks at this part is not occurred, and no water leakage occurred even 12 hours after the test. Also, in the inspection after draining, there was no breakage in the resin coating, and the coating film followed the cracking of the concrete.

Outside surface inside surface

Fig.8 Outside and inside surface at the corner of the leg of wall

Fig.8 shows the peeling of concrete at the corner of the leg and the resin coating on the inner surface. No damage was observed in the resin coating, not only at the wall surface but also at the corner where the damage was large, and no water leakage was observed at the position where the concrete was crushed and peeled off. The major width of crack at R = ± 8/1000 was 0.2 to 0.4 mm, and the total length of wall cracks was about 15m. The maximum crack width was 1.1 to 1.2 mm, and the average crack width was about 0.3 mm.

Relationship Between Shear Force and Total Deformation Angle

The relationship between shear force Q and total deformation angle R is shown in Fig.9. Bending cracking in the test is indicated by □, shear cracking is indicated by ○, and the maximum strength is indicated by ▼. The red line in the figure is the result of FEM analysis performed before loading test using the analysis model shown in Fig.14 below. In this analysis, the material strength of a reinforcing bar and concrete used each standard value. In addition, the blue line in the figure is the calculated value of bending strength by the evaluation formula shown in Japanese guideline of Ref.[2].

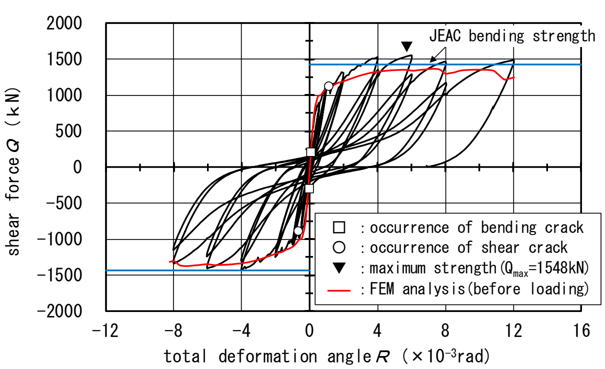

Fig.9 Relationship between shear force Q and total deformation angle R

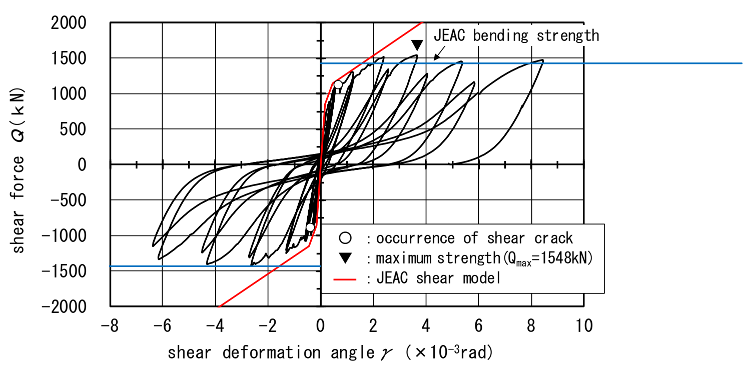

Fig.10 Relationship between shear force Q and shear deformation angle γ

After bending cracking at R of ± 0.5 / 1000, longitudinal bars at the flange leg on the tension side was yield at 1/1000, and that of the horizontal bars of web was at ± 4/1000. The maximum shear force Qmax was confirmed when R was 6/1000, and it was 1548 kN, which was almost the same as the calculated value of bending strength according to the design formula of JEAG 4601[2]. Although the cracks on the flange and web surface expand and develop after the maximum strength, no clear shear failure occurs, and the strength gradually decreases to the final displacement of 12/1000. From these failure processes, it can be said that the failure type in this test is bending failure. When the FEM analysis results and the test results are compared, the relationship between the shear force and the deformation angle almost agrees with the test results, although the maximum shear force in the analysis under plus side force is slightly lower than the test value.

The relationship between shear force Q and shear deformation angle γ is shown in Fig.10. The shear deformation is a value obtained by subtracting the bending deformation and the rotational deformation from total deformation of the wall. The rotational deformation was calculated from pull-out displacement of the vertical rebar of the wall from the base stub. The bending deformation angle was calculated from the vertical deformation of the wall measured on both sides of the test specimen. The ratio of shear deformation, bending deformation and rotational deformation to total deformation is shown in Fig.11.

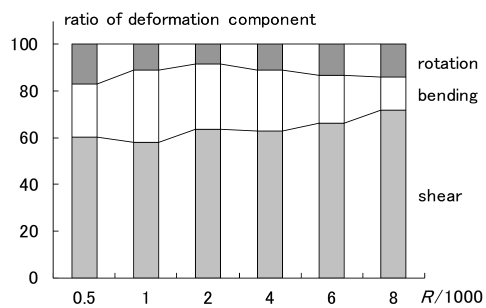

Fig.11 Ratio of deformation component

Evaluation of Crack Width and Crack Interval

As a method to estimate the amount of water leakage from a shear wall when the cracks have occurred due to seismic force, there is a previous study that determined the relationship between the shear deformation angle of the shear wall and the crack width from tests. In this study, it is shown that the following relationship exists for shear stress τ, shear deformation angle γ, crack interval and crack width.

(1) The maximum crack width during loading almost linearly with the increase of γ, and a regression equation is proposed for the relationship between the crack width and γ.
(2) The average crack interval decreases with the increase of γ, and its value asymptotically approaches the rebar interval.

In this section, we will evaluate the shear cracks in the web wall in the same way as the previous literature. The relationship between the maximum crack width and the shear deformation angle γ obtained in this test is shown in Fig.12. The figure shows the peak point and unloading point at each displacement stage, and a regression equation is shown in the figure.

Although the maximum crack width increases with the increase of γ, it tends to plateau at around $\gamma = 4 \times 10^{-3}$. In addition, the maximum crack width in actual wall at γ＝2/1000, which is the design criteria, is about twice the crack width at γ ＝ 2/1000 obtained from the test, and the value is about 1.5 mm. Although the maximum crack width at unloading is smaller than that at loading, the increase of the crack width with respect to the increase of γ shows almost the same tendency as at the peak, but it is constant when γ is 4×10^{-3} or more.

The relationship between the average crack width and the shear deformation angle γ is shown in Fig. 13 for all cracks generated on the wall surface at loading and unloading.
The increase of the average crack width with respect to the increase of the shear deformation angle was smaller than the maximum crack width, and the crack width at unloading was a substantially constant value regardless of the shear deformation angle.

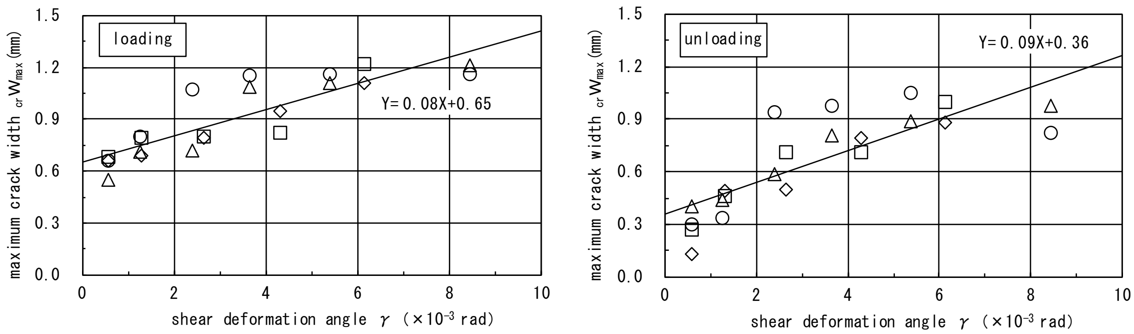

Fig.12 Relationship between the maximum crack width and the shear deformation angle γ

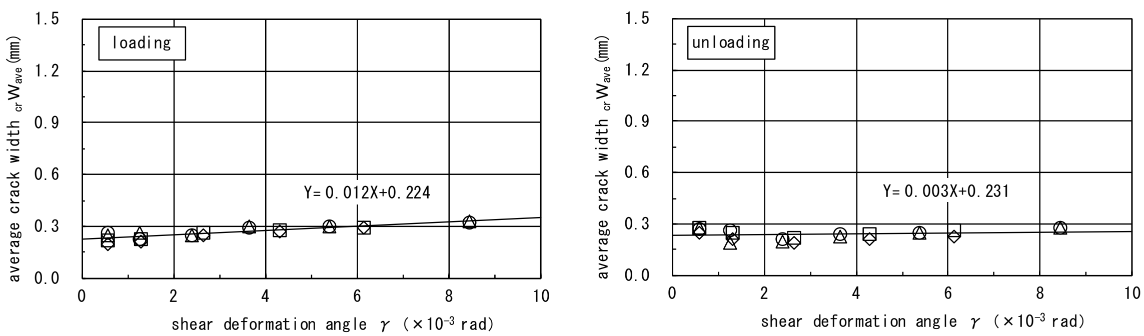

Fig.13 Relationship between the average crack width and the shear deformation angle γ

COMPARISON OF NON-LINEAR FEM ANALYSIS

Analytical Method

Reversed cyclic loading analysis was performed using the analysis model shown in Fig.14. For the material properties of concrete and rebar in analysis, material test results are used. The code used for the analysis is the non-linear program DIANA Version 10.2. A nonorthogonal multidirectional crack model (Maekawa-Fukuura model Ref.[4]) was used as the constitutive law of concrete. The elements used are a 4-node shell element for the wall and an 8-node solid element for the base stub and the stiff top. The rebars were modeled by embedded rebar element and completely bonded to concrete. Coatings are not considered in the model. The order of analysis was to apply dead weight and water pressure, and then give displacement increment to the node in the center of the stiff top to give the same loading history as the test.

Crack Pattern of Analysis

Fig.15 shows the crack pattern at R = +8/1000 and -8/1000, and Fig.16 shows the width of the crack obtained from the analysis. In this analysis, the crack width cannot be obtained directly from the analysis because a smeared crack model is used, but the value shown here assumes that one crack is contained in one concrete element and further that the all strain in the direction orthogonal to the crack becomes the crack width.

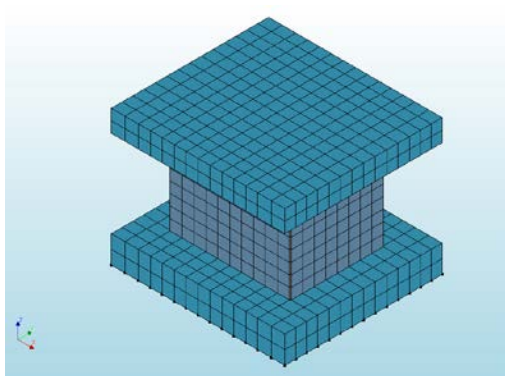

Fig.14 Analytical model

Q-R Relationship and Q-γ Relationship

When comparing Fig.5 and Fig.6 showing the crack width by the test and Fig. 15 and Fig. 16 of the analysis, the analysis value can well simulate the test value for the crack angle and the crack width. In addition, comparing the test value and analysis value for the maximum value of the crack width, the maximum crack width obtained from the analysis is 2.6 mm at R of +8/1000 and 1.8 mm at R of -8/1000, which is larger than the maximum value of 1.2 mm in the test. One of the reasons that the width is larger in the analysis is considered that all elastic strain of concrete between cracks is also supposed to be included in the crack width.

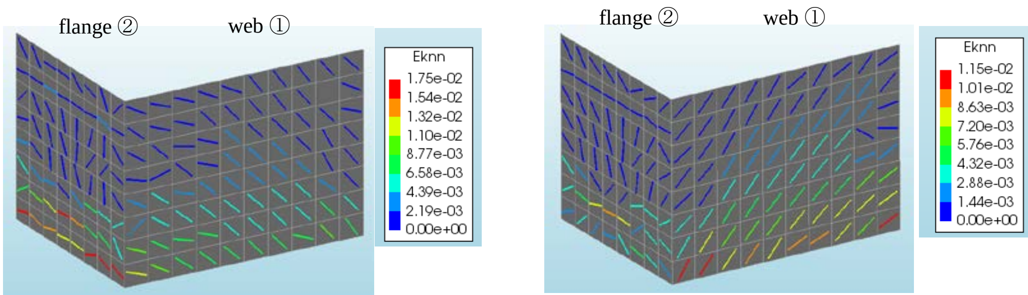

R=+8/1000 R=-8/1000

Fig.15 Crack pattern of analysis

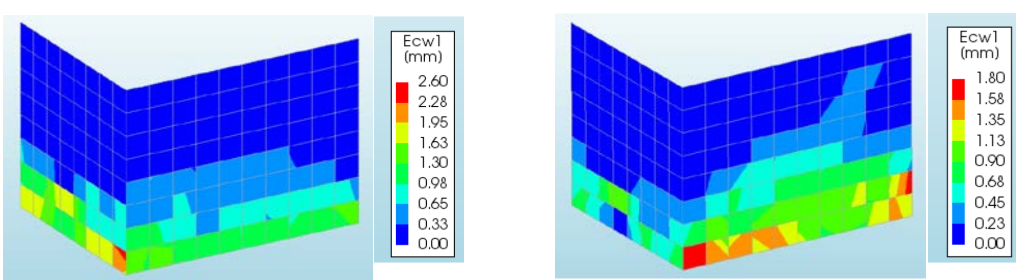

R=+8/1000 R=-8/1000

Fig.16 Crack width of analysis

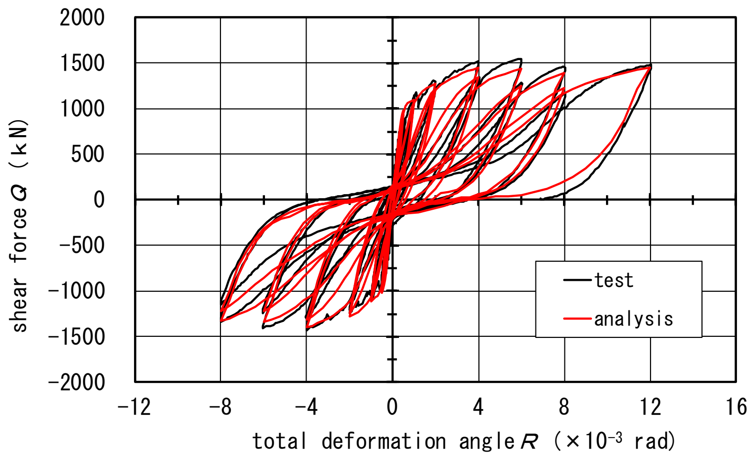

Fig.17 Comparison of Q and R relation with test and analysis

The relationship between shear force Q and overall deformation angle R obtained by analysis is shown in Fig.17 in comparison with the test results. The analytical values are almost consistent with the test results for the maximum load capacity and the hysteresis characteristics of loading and unloading. From these results, it is considered that the behavior of the box wall subjected to water pressure and horizontal force can be well simulated by the modeling method and the material constitutive model used in our FEM analysis.

CONCLUSION

With the box wall coated with high-performance aromatic resin on the inside filled with water, reverse cyclic loading test corresponding to seismic force was conducted to carry out a verification test on water tightness of the water tank. In addition, the relationship between the width and the interval of the crack generated on the wall in this test and the horizontal deformation angle was evaluated. Furthermore, simulation analysis by non-linear FEM analysis was carried out. The obtained findings are described below.

(1) In pit coated with high-performance aromatic resin on the inside, no leaked water from cracks was observed even for deformation beyond the earthquake deformation assumed in the design, and after about 12 hours of drainage the water tightness was maintained also. In addition, no breakage occurred in the resin coating in the inspection after draining.
(2) The maximum crack width increases with the increase of the shear deformation angle until the shear deformation angle γ reaches 4×10^{-3}, but after that the value becomes almost constant. The tendency was almost the same for loading and unloading.
(3) The average crack width was almost constant regardless of the value of shear deformation angle for both loading and unloading.
(4) The behavior of the box wall subjected to water pressure and horizontal force can be accurately simulated by the nonlinear FEM analysis method used in this research.

REFERENCES

[1] Inada, Y., Okada, T., Akino, K., Koike, K., “Study on Shear Cracking Behavior of Reinforced Concrete Shear Walls”, *Summaries of technical papers of Annual Meeting of Japan concrete Institute*, Vol.10，No.3，pp.385-390，1988 (in Japanese)
[2] Nuclear Standards Committee of Japan Electric Association, *Technical Guidelines for Aseismic Design of nuclear Power Plants*, JEAG4601-1991 Supplement 1991

[3] Horiguti, K., Suzuki, M., Honzawa, M., Sakamoto, J., “R&D of Quantitative Evaluation System of Cracks on Distant Slabs by Digital Image Analysis Technology”, *Concrete Journal*, Japan concrete Institute, Vol.56, No.1, pp106-111, January,2018 (in Japanese)

[4] Maekawa, K., Pimanmas, A., Okamura, H., *Nonlinear Mechanics of Reinforced Concrete*, SPON Press, 2003